

Assessment of drought conditions over Vietnam using standardized precipitation evapotranspiration index, MERRA-2 re-analysis, and dynamic land cover

Manh-Hung Le ^{a,*}, Hyunglok Kim ^a, Heewon Moon ^b, Runze Zhang ^a, Venkataraman Lakshmi ^a, Luong-Bang Nguyen ^c

^a Department of Engineering Systems and Environment, University of Virginia, Charlottesville, VA, 22904, USA

^b Institute for Atmospheric and Climate Science, ETH Zurich, Zurich, Switzerland

^c Faculty of Water Resources Engineering, Thuyloi University, Hanoi, Viet Nam



ARTICLE INFO

Keywords:

Hydrology
Drought
MERRA-2
Trend analysis
Land cover

ABSTRACT

Study region: Vietnam.

Study focus: In recent years Vietnam has experienced historical drought events possibly affected by climate change, but the analysis is challenging due to lack of necessary observations for monitoring drought conditions. The goal of this study is to analyze the characteristics of droughts over a 30-year period, using three spatial-resolution MERRA-2 datasets in Vietnam. The Standardized Precipitation Evapotranspiration Index (SPEI) was used as an index for drought based on precipitation and temperature. We also estimated the impacts of drought on agriculture using annual land cover datasets.

New hydrological insights for the regions: Our results identified significant increasing trends in precipitation in Northern Vietnam and decreasing trends in Southern Vietnam. The increasing trends in temperature occurred mainly in Southern Vietnam. These trends in rainfall and temperature resulted in an increasing trend in drought frequency and severity in Southern Vietnam, especially in the South-Central Region and the Mekong Delta. The comparison between the observed drought records and modeled drought index demonstrated that the simulated drought conditions are better at higher spatial resolution. The area under drought in agricultural lands calculated using dynamic land-cover data sets resulted in a better agreement with observed records. Our findings reveal the feasibility of using a model-based drought index in data-sparse areas for long-term trend drought analysis, and for practical applications of advanced re-analysis products in water resource management.

1. Introduction

The slowly evolving nature of drought and its multiple drivers contribute to the various definitions adopted for different purposes and diverse conclusions in identifying the trends under changing climate (Dai, 2011; Van Loon et al., 2016). While a global trend of drought over the last century remains debatable (Greve et al., 2014; Orlowsky and Seneviratne, 2013; Sheffield et al., 2012), some

* Corresponding author.

E-mail address: hml5rn@virginia.edu (M.-H. Le).

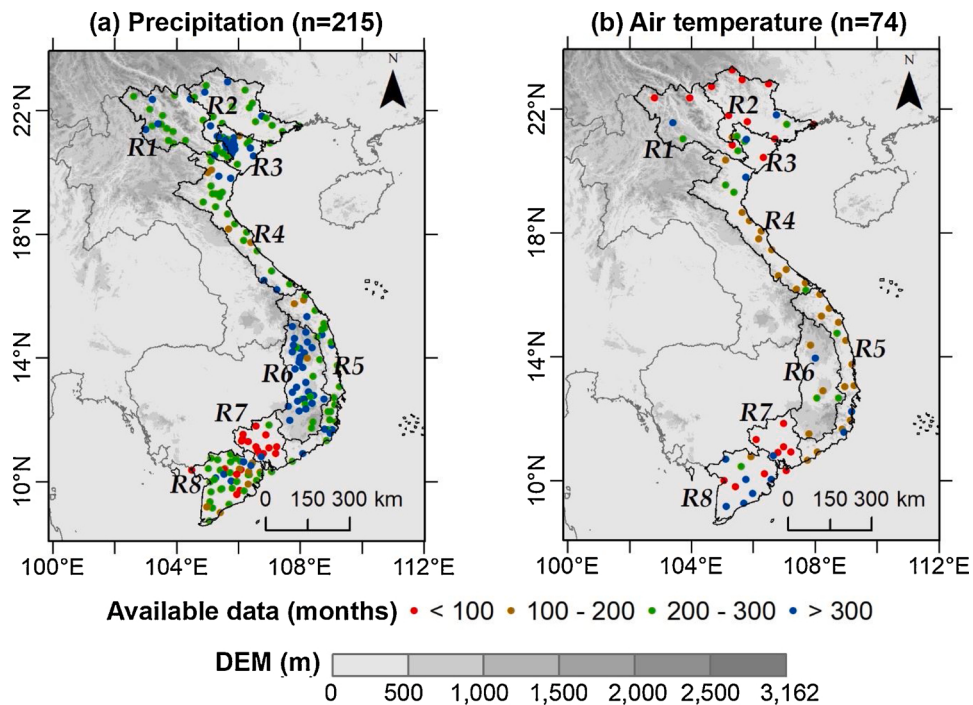


Fig. 1. Boundaries of eight sub-regions (R1-R8) in Vietnam and data lengths of in-situ precipitation and temperature stations.

regions of the world have observed robust tendencies that droughts are becoming more frequent and severe. Drying trends were found in equatorial Africa (Diem et al., 2014; Kawase et al., 2010), South Asia (Krishnan et al., 2016), and the Mediterranean (Hoerling et al., 2012; Valdes-Abellán et al., 2017) in contrast to wetting trends in high latitude regions (Sheffield and Wood, 2008; Zhang et al., 2013). Notably, in recent years several extreme droughts have been observed - California (Ganguli and Ganguly, 2016; Mazdiyasni and AghaKouchak, 2015), Australia (Herold et al., 2016), China (Yuan et al., 2019), Europe (Miralles et al., 2019), and India (Sharma and Mujumdar, 2017). These droughts occurred concurrently with extreme heatwaves, causing severe socioeconomic and ecological damages and are likely to occur with increased frequency. Such possibly intensified impacts of drought, compounded by its intricate characteristics, demands a substantially improved quality of observations for proper monitoring and management in many regions of the world.

While impacts of varying temporal scales on the efficiency of drought indices are well-documented (Raziei et al., 2013; Zhu et al., 2016; Zuo et al., 2018), only a few studies have investigated the performances of drought indices at different spatial scales. Golian et al. (2019) found that the values of Critical Success Index (CSI) derived from products of Multi-Source Weighted-Ensemble Precipitation (MSWEP) at coarser resolution (0.5° and 1°) as significantly lower skill in drought detection for severe drought events compared to the CSI computed from the MSWEP data at 0.1° . Additionally, Raziei et al. (2013) demonstrated that the dependence of the spatial patterns of droughts on time scales increased when using higher spatial resolution data. In light of this, it seems that the drought indices computed from the high-resolution data have greater potential to accurately describe the spatial characteristics of drought conditions than those derived from coarser-resolution data. Previous studies have focused on drought indices based on the data sets with relatively coarser-resolution (e.g., larger than 10 km), while the analyses that assess the performance of the drought indices at finer spatial resolutions (e.g., less than 10 km) have seldom been studied.

Drought risk in agricultural regions is essential information; however, this information is currently limited by using static datasets. For example, when Rojas et al. (2011) and Winkler et al. (2017) investigated agricultural areas affected by drought, they only used a typical year to represent land cover for the entire study period. However, land cover, especially for agricultural land, is subjected to change over time due to international trade, climate adaptation, urbanization, industrialization, food security and economic policies (Rutten et al., 2014). Therefore, in order to accurately evaluate drought conditions in agricultural locations, it is required to use a dynamic land cover database to reflect spatial changes in land cover over time. To the best of our knowledge, previous studies have not used dynamic land cover for drought assessment.

In this study, we aim to examine three hypotheses, viz. - (1) Does high spatial resolution data detect drought trends better than low spatial resolution data? (2) Does high spatial resolution data have advantages of capturing drought events better than low spatial resolution data? (3) Does dynamic land cover provide better information on agricultural lands affected by drought over the years? We selected the country of Vietnam as a case study to test our hypotheses. Firstly, drought investigation is of paramount importance for Vietnam as this disaster ranked third among economic losses amongst natural hazards in the country (Nguyen and Shaw, 2011). Secondly, most of the studies which assessed droughts in Vietnam are either based on sparsely distributed in-situ observations (Le et al., 2019b; Vu-Thanh et al., 2014) or relatively coarse spatial resolution data (Vu and Mishra, 2016; Vu et al., 2018). Therefore, high

Table 1

Descriptive statistics of precipitation and air temperature from MERRA-2 and in-situ data in eight sub-regions. The MERRA-2 data were extracted at the same in-situ locations.

Annual Precipitation	In-situ			MERRA-2		
	Max (mm)	Min (mm)	Mean (mm)	Max (mm)	Min (mm)	Mean (mm)
R1 (n = 25)	2,411	1,129	1,764	1,563	939	1,352
R2 (n = 18)	3,775	1,170	1,775	1,481	1,231	1,361
R3 (n = 25)	1,793	1,239	1,533	1,502	1,374	1,453
R4 (n = 24)	3,889	1,320	2,063	2,122	1,342	1,604
R5 (n = 27)	3,738	841	2,069	2,140	1,166	1,532
R6 (n = 36)	2,538	1,267	1,834	1,602	834	1,100
R7 (n = 16)	2,779	1,288	1,914	1,496	1,175	1,369
R8 (n = 44)	2,459	809	1,628	2,006	1,124	1,569

Annual Air Temperature	In-situ			MERRA-2		
	Max (°C)	Min (°C)	Mean (°C)	Max (°C)	Min (°C)	Mean (°C)
R1 (n = 6)	24.6	23.1	24.0	23.0	20.0	21.3
R2 (n = 10)	24.4	20.7	22.9	23.2	18.9	21.2
R3 (n = 5)	24.2	23.6	23.9	23.9	23.0	23.4
R4 (n = 14)	25.1	21.9	24.2	25.1	21.7	23.6
R5 (n = 15)	27.5	24.6	26.5	26.3	24.2	25.0
R6 (n = 6)	25.2	21.8	23.2	24.5	21.9	23.5
R7 (n = 7)	28.2	26.0	27.1	27.3	26.4	26.8
R8 (n = 11)	28.0	27.0	27.4	27.5	26.7	27.0

spatial resolution drought datasets are unexplored in Vietnam. Moreover, we can obtain annual land cover information for Vietnam for the past 30 years from SERVIR-Mekong land use land cover portal. This land cover database could enable us to examine our third hypotheses mentioned above.

This study selected the Standardized Precipitation Evapotranspiration Index (SPEI) (Vicente-Serrano et al., 2010) to estimate drought conditions in Vietnam. This index is an appropriate drought index in examining changes in droughts under global warming (Le et al., 2019a; López-Moreno et al., 2013; Wang et al., 2018), and in representing different drought types such as meteorological, agricultural, hydrological, and socioeconomic droughts (Chen and Sun, 2015). We estimated the SPEI at three spatial resolutions (1-, 9- and 36-km) using precipitation and air temperature from the second Modern-Era Retrospective analysis for Research and Applications (MERRA-2). One of the main reasons that we chose MERRA-2 is that the data has been widely validated, showing good performance globally. Readers will find representative research at <https://gmao.gsfc.nasa.gov/reanalysis/MERRA-2/pubs/>. Furthermore, as MERRA-2 is open to the public and allows the downloading of near-real-time data, it has great potential for practical application in drought analysis. To investigate agricultural drought areas, we extracted agricultural land cover in each year from SERVIR-Mekong land use land cover database, and re-sampled the data to 1-, 9-, and 36-km. To explore the possible trends in a time series, we applied the Mann-Kendall test, which is commonly used to detect trends in hydro-meteorological time series (Joshi et al., 2019; Mondal et al., 2015; Velpuri and Senay, 2013).

This study is organized as follows. Section 2 introduces the Study Area. Section 3 presents the Datasets. Section 4 presents the Methodology. Results and Discussions, and Conclusions are presented in Section 5 and Section 6, respectively.

2. Study area

Vietnam has a total area of 331,212 km², extending from 8.2 °N – 23.5 °N, 101.1 °E – 110.3 °E, and a home of more than 95 million people (In 2018 ranked 15th in global population). In order to assess drought condition in Vietnam, previous studies often divided it into seven subregions that are based on differences in climatic conditions (Le et al., 2019b; Vu et al., 2018). This study, however, divided Vietnam into eight sub-regions based on a sub-national administrative level. This allows for easy comparison with existing agricultural drought statistics. These eight sub-regions are Northwestern Region (R1); Northeastern Region (R2); Red River Delta (R3); North Central Region (R4), South Central Region (R5); Central Highlands (R6); Southeastern Region (R7); and the Mekong Delta (R8) (Fig. 1).

3. Data sets

3.1. Ground observations

This study collected monthly data from 215 precipitation stations and 74 temperature stations from multiple sources, including Vietnam Meteorological and Hydrological Administration (VMHA), Mekong River Commission (MRC), and Japan International Cooperation Agency (JICA) (Fig. 1). All data has passed quality checks. We used these in-situ observations to compare with precipitation and air temperature from MERRA-2 datasets. Data availability at each station varied between 40 and 360 months (Fig. 1). Descriptive statistics of observed precipitation and air temperature in each sub-region can be found at Table 1. Also, mean elevation

Table 2

Mean elevation and Gini-Simpson index ([Simpson, 1949](#)) in eight sub-regions. The Gini-Simpson index is calculated to reflect heterogeneity of surface land for each sub-region. Higher Gini-Simpson index corresponds to greater variation in land surface.

Sub-region	R1	R2	R3	R4	R5	R6	R7	R8
Mean Elevation (m)	801.6	387.1	22.3	298	334.4	660.5	89.4	3.9
Gini-Simpson Index	0.939	0.92	0.451	0.926	0.933	0.914	0.897	0.015

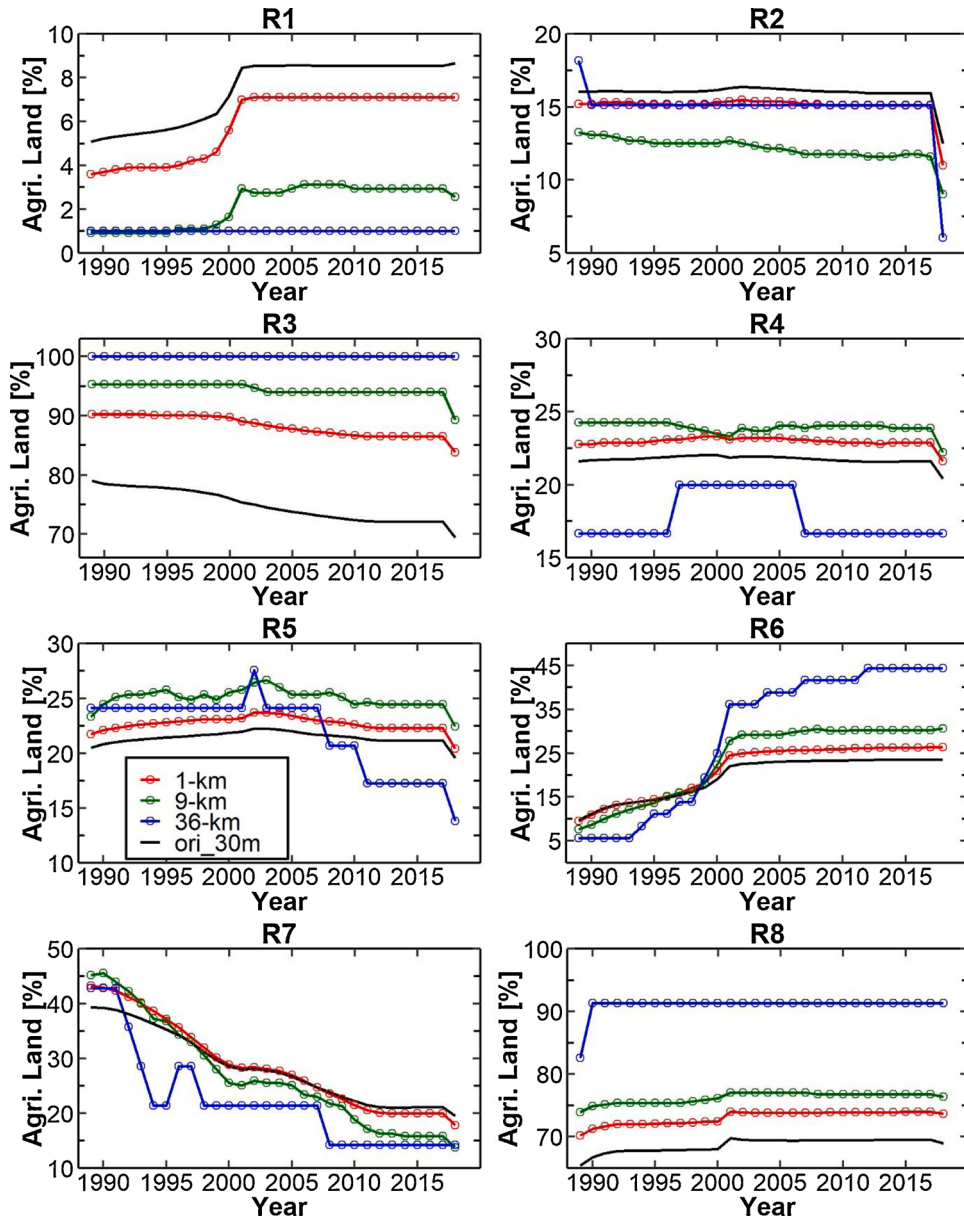


Fig. 2. Percentage of agricultural land based on different spatial resolutions in eight sub-regions during 1989–2018. The black line is the agricultural land area derived from the 30-m original land cover dataset.

and Gini-Simpson index are presented in [Table 2](#) for eight sub-regions.

We obtained 1989–2014 data on agricultural land affected by drought for the R4 and R5 regions from the Vietnamese Ministry of Agriculture and Rural Development (MARD). The Decree No.01.2008/ND-CP on responsibilities, tasks, authorities and organization structure of MARD: “Ministry of Agriculture and Rural Development is a state agency, carrying out tasks of state management on such fields as agriculture, forestry, salt industry, aquaculture, water resource and rural development in the country; of state management on public services

and fields under the management of the Ministry". The MARD has its department located in each province through Vietnam. Officials from these departments conduct annual surveys on agricultural activities lands within their provinces to obtain statistical records on natural disasters and the development of these activities.

3.2. The Modern-Era Retrospective Analysis for Research and Applications, Version 2 (MERRA-2)

The Modern-Era Retrospective Analysis for Research and Applications, version 2 (MERRA-2), is the latest atmospheric reanalysis of the modern satellite era produced by NASA's Global Modeling and Assimilation Office (GMAO). The goals of MERRA-2 are to provide a regularly-gridded, homogeneous record of the global atmosphere, and to incorporate additional aspects of the climate system (Gelaro et al., 2017). The superior feature of MERRA-2 over its predecessor, MERRA, is that it assimilates several observation types and includes updates to the Goddard Earth Observing System (GEOS) model and analysis scheme; this allows it to provide a feasible ongoing climate analysis. MERRA-2 includes ground-based remotely sensed data and numerous satellite observations both before and after the introduction of NOAA-18 satellite in 2005. The complete set of input observations assimilated in MERRA-2 is summarized in Gelaro et al. (2017) and detailed description of these data uses shown in McCarty et al. (2016). In this study, the bilinear transform was used to produce 0.01×0.01 ($\sim 1\text{-km}$), 0.09×0.09 ($\sim 9\text{-km}$), and 0.36×0.36 ($\sim 36\text{-km}$) spatial resolutions of MERRA-2-derived precipitation and air temperature forcing data using the Land surface Data Toolkit (LDT) (Kumar et al., 2006). For further information regarding LDT, please refer to Arsenault et al. (2018); and visit <https://lis.gsfc.nasa.gov>.

3.3. Agricultural land cover dataset

High resolution (30 m) land cover data for Vietnam during 1989–2018 were obtained from the land-cover portal website maintained by SERVIR-Mekong (<https://rlcms-servir.adpc.net/en/landcover/>). This system provides consistent land cover products at regular intervals, with quality control from multiple sources. Based on these yearly land cover data, we determined agricultural land areas (sum of croplands and rice paddies from SERVIR-Mekong's classification) and calculated the area percentage of drought on a monthly basis. This work enables us to precisely estimate drought areas for agricultural regions only and not for other land covers. Since we used MERRA-2 datasets with three different spatial resolutions (1-, 9-, and 36-km), the land cover datasets were also resampled from 30 m to these corresponding resolutions.

The temporal percentage change of agricultural land in Vietnam at three spatial resolutions is given in Fig. 2. The R3 and R8 are two deltas corresponding to the two largest river basins in Vietnam - Red-Thai Binh River and Mekong River, respectively. Therefore, agricultural lands in these regions account for a large proportion of the total land over the years. For 30 years, agricultural land in R7 experienced a significant reduction while that land in R6 exhibited a considerable increase. Comparing agricultural land estimated from three spatial resolutions (1-, 9-, and 36-km), higher spatial resolution land cover datasets seem to have smoother inter-annual changes over 1989–2018, and to be closer with these figures of original land cover dataset (Fig. 2). Different agricultural land resolution datasets can result in a significant difference in percentage of total agricultural land. For example, in R8, the agricultural land was around 90 % of the total land with a 36-km land cover dataset but 73 % with the 1-km land cover dataset. The large inhomogeneous distribution of land cover is probably a result of the different agricultural land estimations given when we used different spatial resolutions. An example of agricultural land in R3 in different spatial resolutions is given in Supplementary 1.

In short, the agricultural land in Vietnam exhibited a great variation in both temporal and spatial scales. Therefore, drought evaluation in agricultural land in Vietnam requires a rigorous information for a better estimate.

4. Methodology

4.1. Temporal trend analysis

The Mann-Kendall (MK) test was performed to analyze the trends of precipitation, temperature, and drought conditions. The MK test is a non-parametric test that statistically assesses the monotonic trends in data over time (Hirsch and Slack, 1984; Kendall, 1938; Mann, 1945). We selected this non-parametric test because our data sets are not normally distributed, and this test is distribution-free (Gocic and Trajkovic, 2014). For purpose of robustness, in the presence of autocorrelation time series which could affect trend interpretation results (Yue et al., 2002), we removed the serial correlation effect using the pre-whitening method before applying the MK test (Gocic and Trajkovic, 2014). Then, the Sen's slope (Sen, 1968) was used to examine the magnitude of trends.

4.2. Characteristics of drought dynamics

From MERRA-2's precipitation and air temperature for each grid cell, we calculated the SPEI throughout Vietnam, at three spatial resolutions - 1-, 9-, and 36-km. We employed three-parameter log-logistic distribution for fitting SPEI. A negative value of SPEI indicates that a particular value of the water-related variable is lower than the median of the total distribution. A drought event occurs when the SPEI value reaches -1 or lower. The water-related time series - SPEI requires a deficit between precipitation (P) and potential evapotranspiration (PET). We calculated PET from air temperature data based on the Thornthwaite method (Thornthwaite, 1948).

In the present study, we used a 3-month timescale, which was estimated by accumulating three consecutive months of P-ET. This 3-month timescale often reflects a shortage of water availability for agricultural uses (Svoboda et al., 2012).

Temporal drought characteristics were analyzed using drought frequency (F) and drought severity (S) (Le et al., 2019b). The details

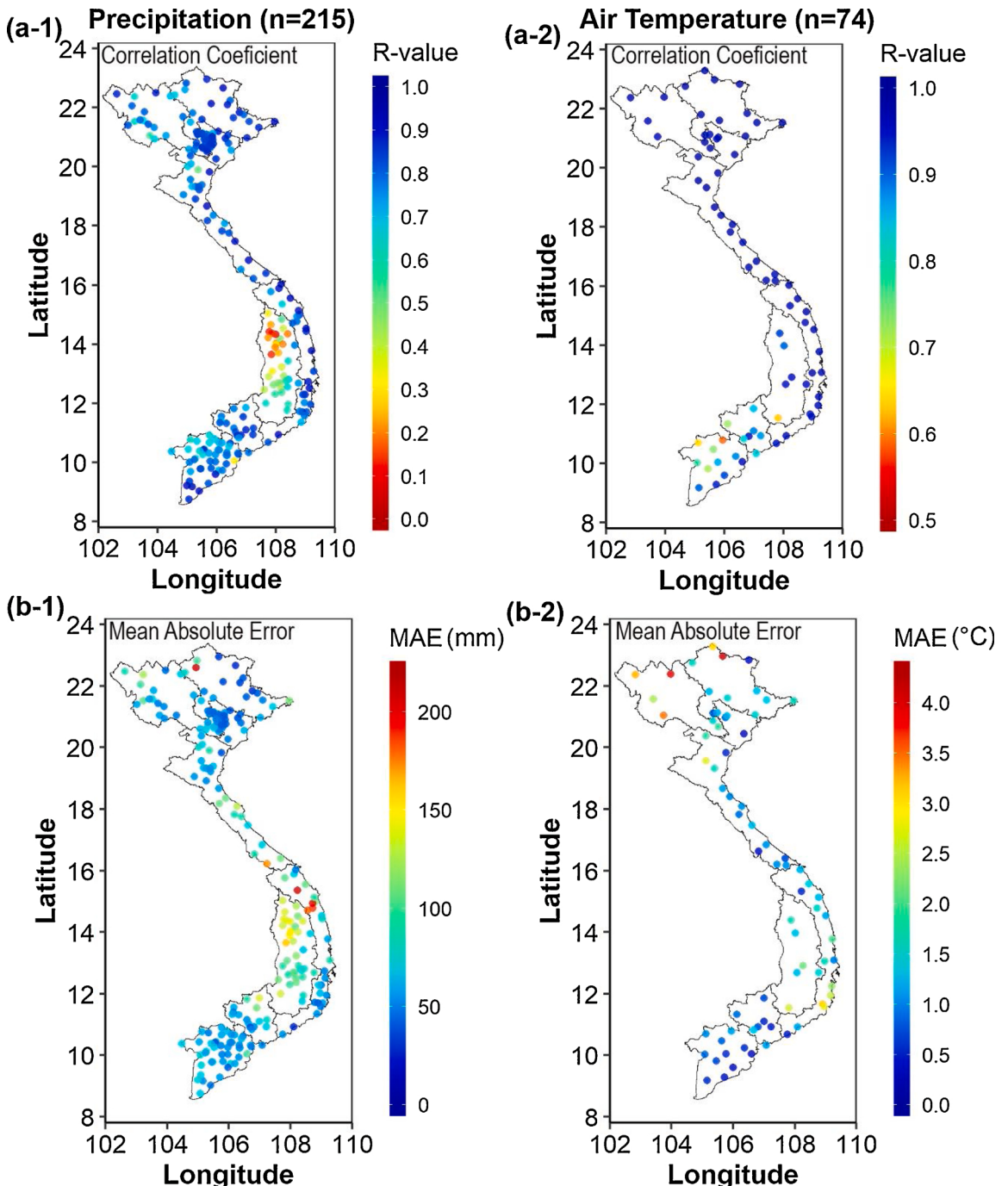


Fig. 3. (a) Correlation coefficient and (b) Mean absolute error between MERRA-2 datasets and observed precipitation (right) and observed air temperature (left).

regarding these drought characteristics are the following Eqs. (1) and (2).

$$F = \frac{\sum_{i=1}^m Du_i}{N} \times 100\% \quad (1)$$

Where Du_i is i th drought duration, which is the number of consecutive months in which the SPEI is below -1; m is the number of drought duration, N is the total months.

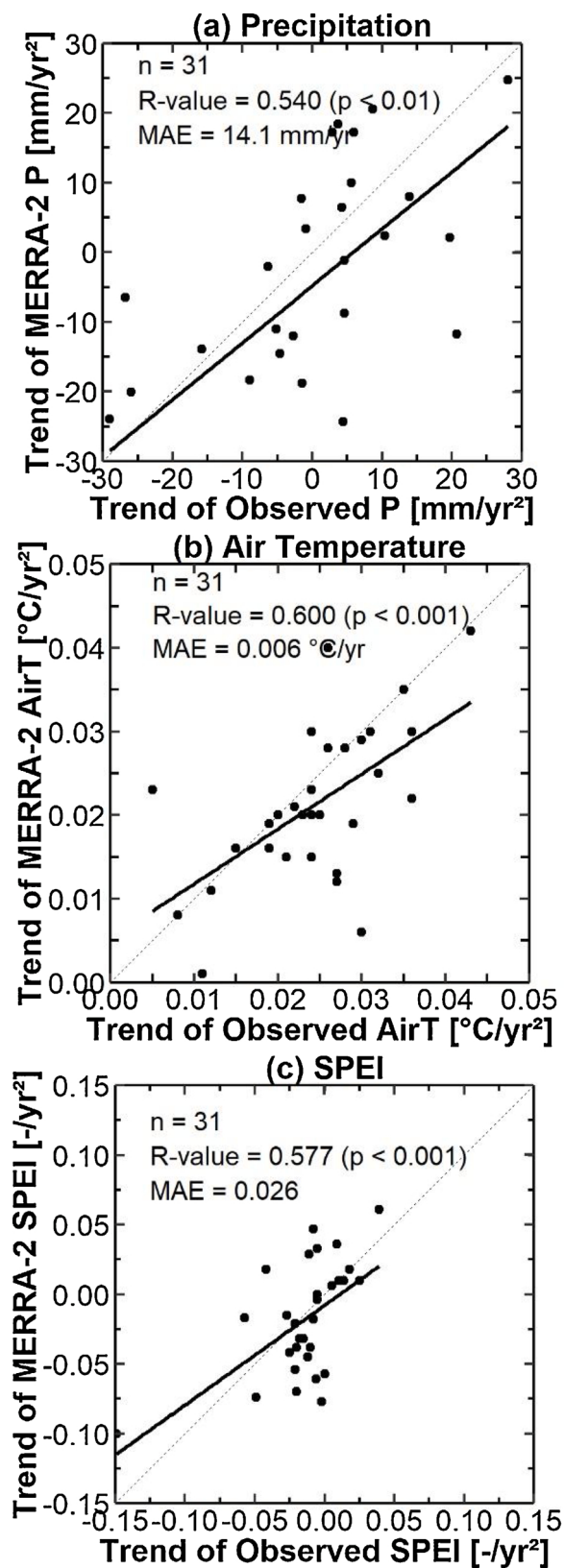


Fig. 4. Validation of the MERRA-2 dataset against observation in (a) comparison of MERRA-2 and observed precipitation Sen's slope, (b) comparison of MERRA-2 and observed air temperature Sen's slope, (c) comparison of MERRA-2 and observed SPEI Sen's slope.

$$S = \sum_{i=1}^{Du} DI_i |DI_i| < -1 \quad (2)$$

Where DI_i is SPEI at month i .

For assessing drought in space, we used a binary approach to represent drought state $Ds(t)$ at time step t for each grid cell as follows:

$$Ds(t) = \{1 \text{ if } DI(t) \leq -1; 0 \text{ if } DI(t) > -1\} \quad (3)$$

Where $DI(t)$ is the value of drought index at time step t .

For a given region, the percentage drought area at time step t , $PDA(t)$ (%), is a ratio between total number cells in drought and the total number of cells in the region N_{total} .

$$PDA(t) = \frac{\sum_{i=1}^{N_{total}} Ds(t) |DI(t)| \leq -1}{N_{total}} \times 100\% \quad (4)$$

We estimated three monthly percentage drought area (PDA) datasets. The first dataset is the percentage drought area for the entire region (hereafter referred to as PDA-E), which is equivalent to the total land area of a region. The second dataset is the percentage of drought area for agricultural land using static land cover (hereafter PDA-AS). N_{total} in the second case is equivalent to total agricultural land of 2005 which represents for the period 1989 and 2018. The cells in drought are counted for the agricultural land in the year of 2005. The third dataset is the percentage of drought area for agricultural land using dynamic land cover (hereafter PDA-AD). N_{total} in the third case is equivalent to total agricultural land of the year i ($i = 1989, 1990, \dots, 2018$). The cells in drought are counted for the agricultural land each year. We compared these three estimated PDAs with record PDAs in R4 and R5 regions. Since the record PDAs datasets are only available annually, we averaged monthly PDAs from our estimations to an annual basis to have the same temporal time step as the actual data.

5. Results and discussion

5.1. Assessment on MERRA-2's precipitation and air temperature in Vietnam

Over our region of interest, there is no prior research of validating MERRA-2 using in-situ measurement; therefore, we conducted a validation study before applying MERRA-2 data for drought analysis. To do that, we extract grid values of MERRA-2 to ground observation points using the nearest neighbor method. We used this method to preserve the values at different spatial resolutions. In total, for each precipitation and air temperature dataset, three comparisons were made between MERRA-2 datasets (1-, 9-, and 36-km) and in-situ measurements. Since the results were found similar in each spatial resolution of MERRA-2 product, this section only presents evaluation results of 1-km MERRA-2 in terms of correlation coefficient (R-value) and mean absolute error (MAE) (Fig. 3). The results of 9- and 36-km MERRA-2 can be found in Supplementary 2.

Generally, precipitation from MERRA-2 exhibited a good agreement with the precipitation from in situ data, with median R-value of 0.809 (Fig. 3.a). The MERRA-2 precipitation exhibited relatively poor correlation with in-situ dataset in Central Highlands (R6), specifically in its northern part. This can probably be attributed to a combination of a typical bimodal South Asian summer monsoon interacting with complex topography (Phan and Ngo-Duc, 2009; Tuan, 2019; Van Der Linden et al., 2016). The MERRA-2 precipitation product itself observed many outlier values in the R6 region (see Supplementary 3). Note that the R1, R2, and R5 regions also have high Gini-Simpson Indices (Table 2) but their monsoon circulation is not as complex as that of the R6 region (Nguyen and Nguyen, 2004). With respect to air temperature, a very good relationship between MERRA-2 and in-situ data was found, with a median R-value of 0.977. Among sub-regions, only the North Mekong Delta (North R8) exhibited a moderate relationship (median R-value of 0.75).

The MAE values between precipitation and air temperature from MERRA-2 and these from in-situ data is given in Fig. 3.b. The median MAE value of precipitation was 57.5 mm. High precipitation MAE values (>150 mm) were found at several stations in north R5 and in northwest R2 (Fig. 3(b-1)). These high values can probably be attributed to the typical local rainfall problem. The stations in these areas are located at the base of mountains (i.e., Truong Son mountains and Tay Con Linh mountains), meaning they receive the highest rainfall amounts in Vietnam (3,500–4,300 mm annually) due to orographic rainfall. With such typical very high rainfall observed, MERRA-2 often underestimates the rainfall during the rainy season. Previous studies also revealed large underestimation of satellite-based and re-analysis rainfall datasets in Central Vietnam where observed rainfall is extremely high (>3000 mm) (Le et al., 2020). The median MAE values of MERRA-2's air temperature was 1.14 °C (Fig. 3(b-2)). Except for R6, MERRA-2 dataset generally underestimated air temperature over Vietnam (Table 1). This underestimation is similar to the results from re-analysis ERA-4.0 data (Phan and Ngo-Duc, 2009). It may be attributed to the lapse rate due to complex topography.

We further assessed MERRA-2 datasets in terms of trend estimation at 31 stations that have both precipitation and air temperature datasets longer than 15 years. A comparison between MERRA-2 and observed precipitation trend is given in Fig. 4(a). The estimated annual precipitation trend from MERRA-2 exhibited a reasonable agreement with observed values, with a correlation coefficient of 0.540 ($p < 0.01$). The estimated annual air temperature from MERRA-2 demonstrated a slightly better relationship with observed air temperature (R-value = 0.600, $p < 0.001$, Fig. 4(b)). The SPEI which were calculated from precipitation and air temperature at the same location, also exhibited a reasonable relationship between modelled and observed data (R-value 0.577, $p < 0.001$, Fig. 4(c)).

In short, the above results demonstrate that MERRA-2 is adequate to investigate climate change and drought characteristics in Vietnam. Therefore, in the next sections, we will utilize the advantages of the MERRA-2 dataset in characterizing precipitation, air

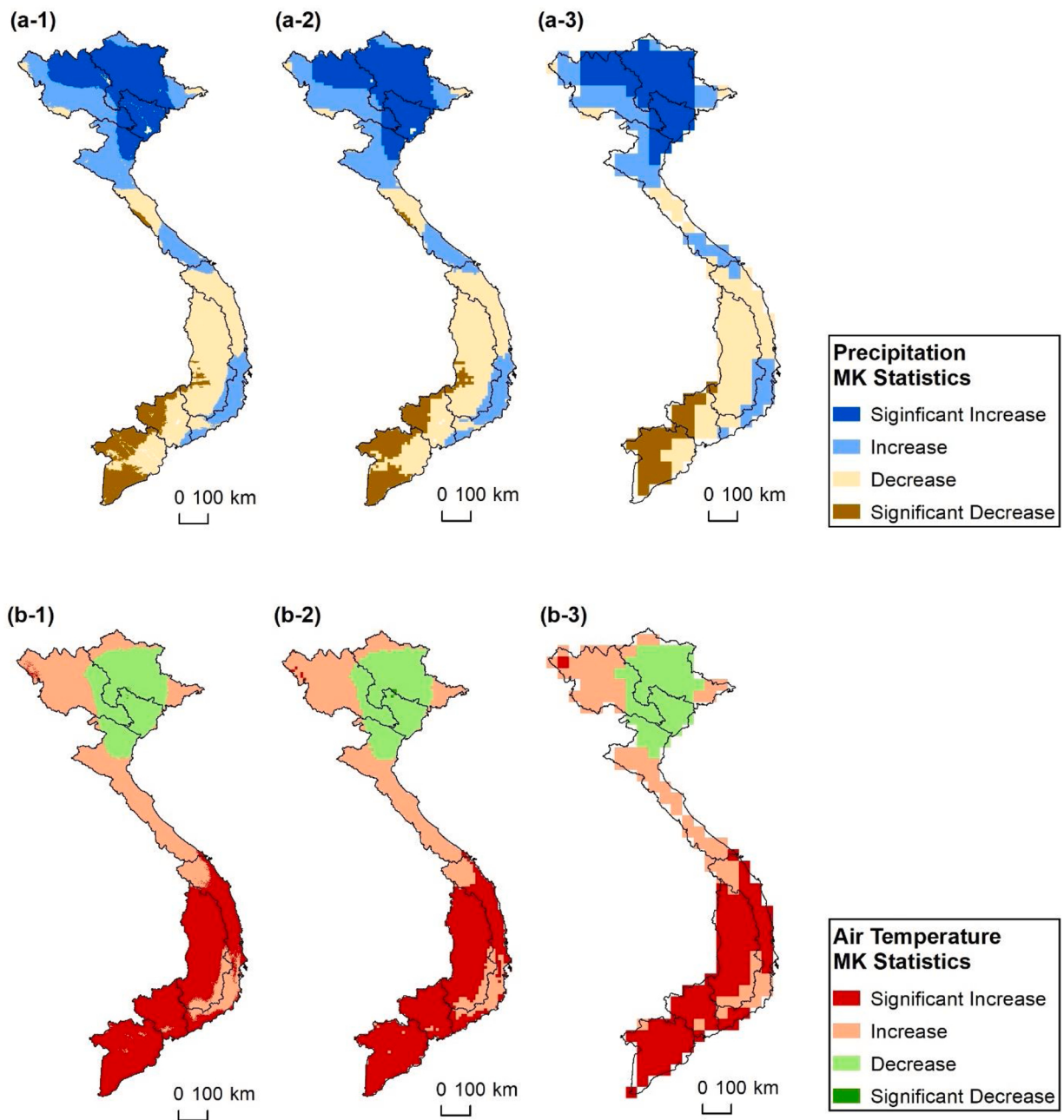


Fig. 5. MK Statistics test of precipitation (upper) and air temperature (lower) during 1989–2018 in Vietnam in different spatial resolutions (1-, 9-, 36-km).

temperature, and drought trends over 30 years in Vietnam.

5.2. Spatial-temporal assessment on precipitation and air temperature characteristics in Vietnam based on MERRA-2 dataset

Thirty-year trends in annual precipitation and air temperature are given in Figs. 5 and 6. Most of the northern parts of Vietnam (R1, R2, and R3) exhibited an increasing trend in precipitation. On the contrary, annual precipitation trends in the south of R6, R7, and R8 declined during the study period. The most significant decreasing trend of annual precipitation can be observed partially in R6, and the northern portion of R5 and a similar decreasing trend over these regions have also been observed during the winter season (Vu and Mishra, 2016).

Overall, the total areas with significant increasing trends in precipitation were 25.7 %, 25.7 %, and 26.5 % in 1-, 9-, and 36-km

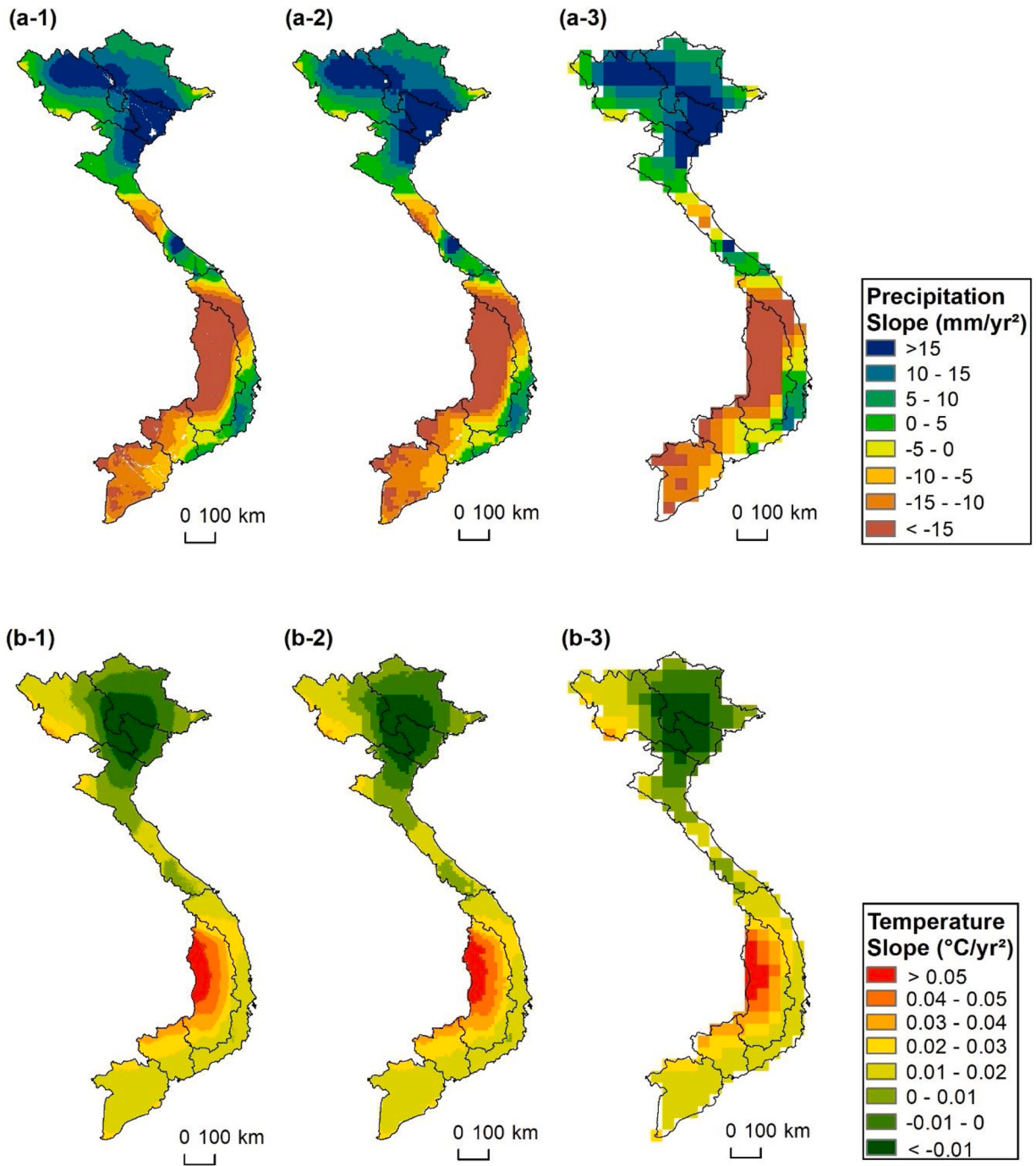


Fig. 6. Sen's slope of precipitation (upper) and air temperature (lower) during 1989–2018 in Vietnam in different spatial resolutions (1-, 9-, 36-km).

resolutions, respectively. Significant decreasing trends in precipitation were also found in 11.4 %, 11.8 %, and 11.8 % of the total area in 1-, 9-, and 36-km resolutions, respectively. Although different spatial resolutions of precipitation and air temperature MERRA-2 products showed similar spatial patterns, the 1-km product provided more detailed spatial variation in trends compared to the other two.

In the past thirty years, the temperature in Vietnam went through a significant increase throughout the country, especially in the southern part (Figs. 5.b and 6.b). The highest increase rate was found in R6. The rapid increase of the temperature in southern Vietnam was also found in Nguyen et al. (2014). Our data show that 40.3 %, 40.5 %, and 40.2 % of the total land area in Vietnam exhibited significant increasing trends based on 1-, 9-, and 36-km products, respectively. Again, the 1-km product could provide more variation

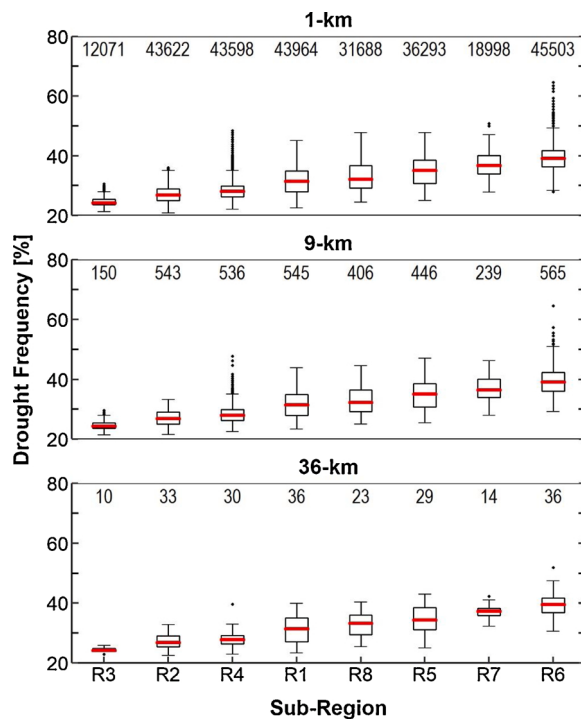


Fig. 7. Regionally averaged drought frequency estimated from SPEI in eight sub-regions of Vietnam in different spatial resolutions (1-, 9-, 36-km). Boxes represent the interquartile range, median, and outliers. The tops and bottoms of each box are the 10th and 90th percentiles of the data. The number on top of each box plot denotes sample sizes for each sub-region.

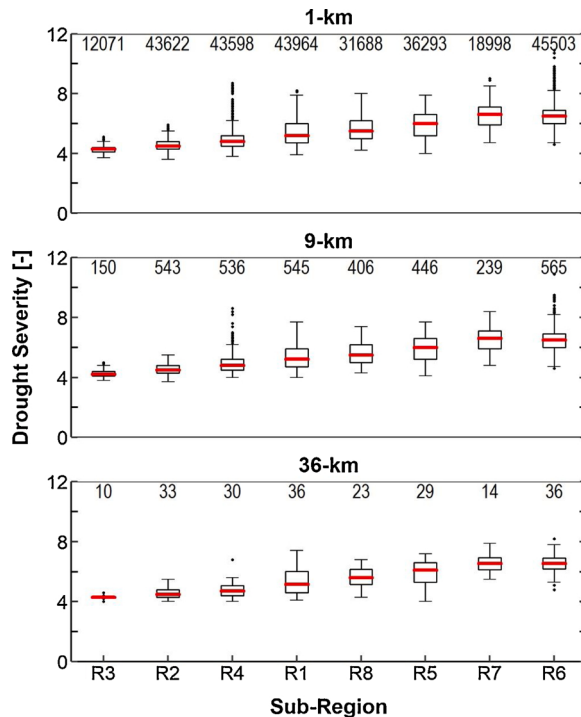


Fig. 8. Regionally averaged drought severity estimated from SPEI in eight sub-regions of Vietnam in different spatial resolutions (1-, 9-, 36-km). Boxes represent the interquartile range, median, and outliers. The tops and bottoms of each box are the 10th and 90th percentiles of the data. The number on top of each box plot denotes sample sizes for each sub-region.

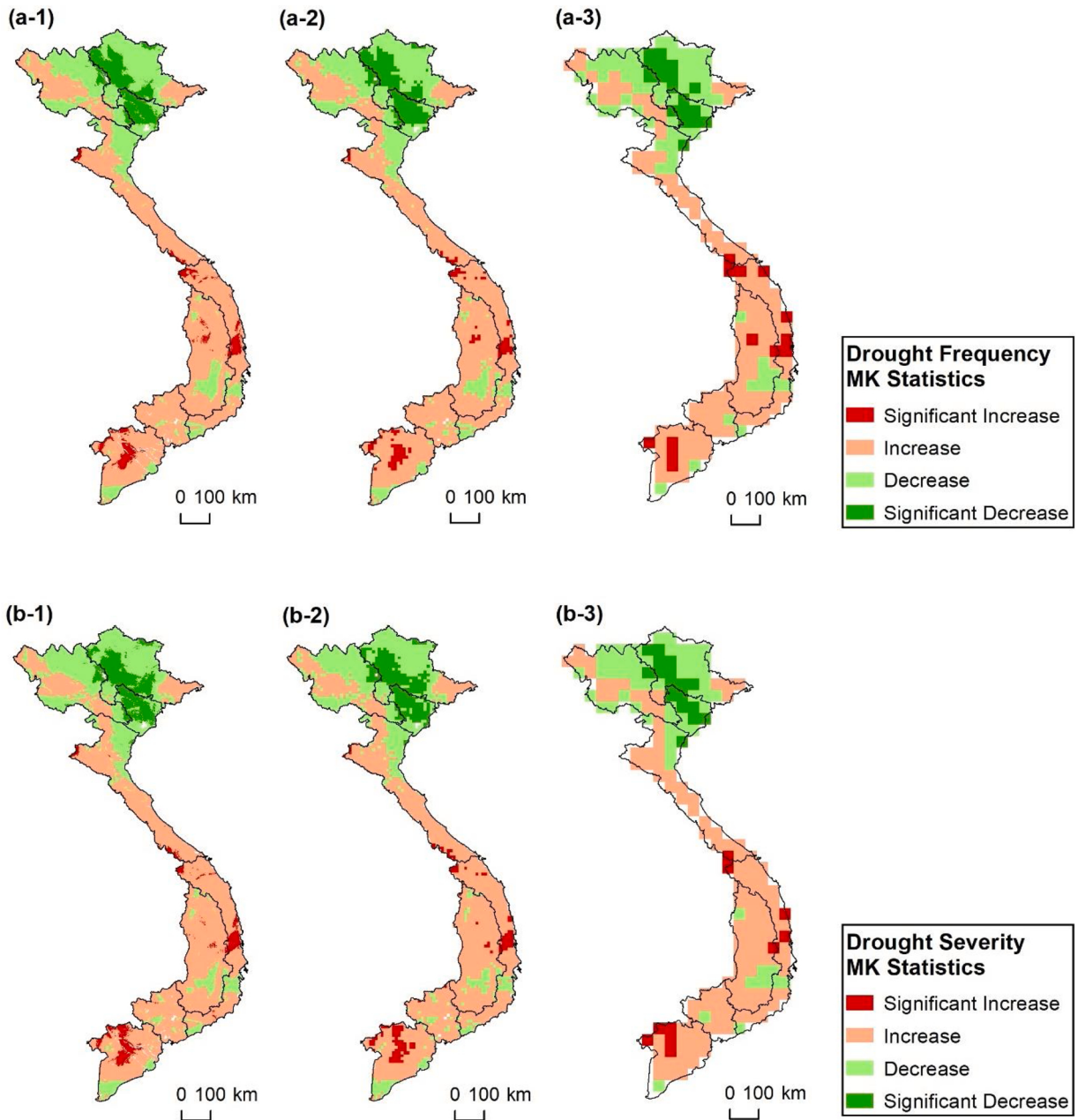


Fig. 9. MK Statistics of drought frequency (upper) and severity (lower) based on SPEI during 1989–2018 in Vietnam in different spatial resolutions (1-, 9-, 36-km).

details in temperature trends than the other two.

5.3. Spatial-temporal assessment on drought characteristics in Vietnam based on MERRA-2 datasets

In this section, we assess drought characteristics and trends for the entire land in each sub-region of Vietnam. Figs. 7 and 8 shows regionally averaged drought frequency and severity for SPEI. Generally, regions with a higher frequency of drought show higher drought severity (in absolute values), inferring a possibly positive correlation between the two metrics of drought. The drought-prone areas were found in the R5, R6, R7 and R8 regions. The drought problems in R5, R6, and R8 were in line with observed records (Hoc, 2002; Ngo et al., 2020; Nguyen and Shaw, 2011). Interestingly, we detected high values in drought frequency and drought severity in R7. However, not many records of droughts were observed in this region by comparison with other regions. The reason that drought is less noticeable in R7 may be that this region primarily cultivates cash crops (e.g., pepper, coffee, rubber, and cashew) which require

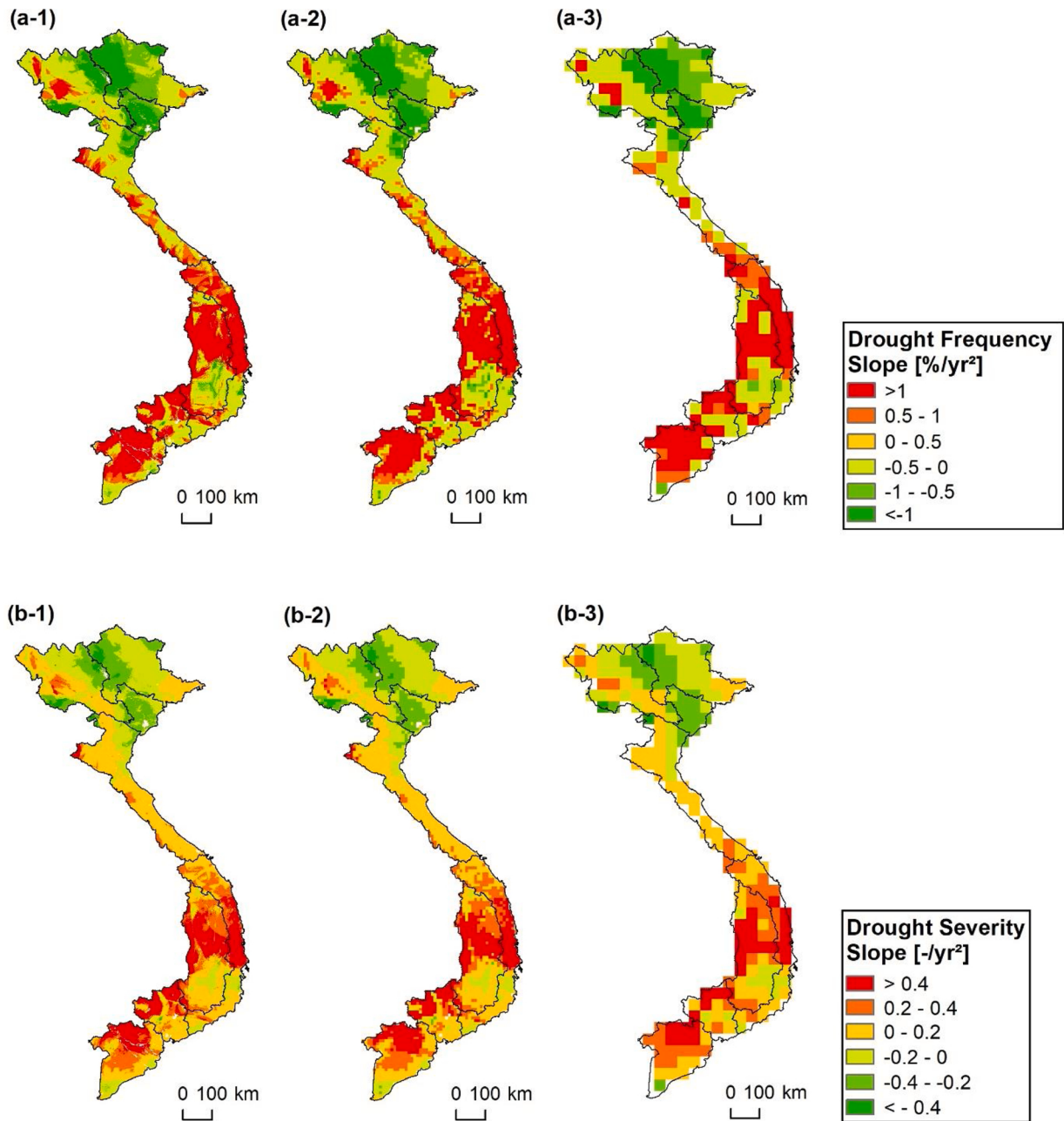


Fig. 10. Sen's slopes of drought frequency (upper) and severity (lower) based on SPEI during 1989–2018 in Vietnam in different spatial resolutions (1-, 9-, 36-km).

less water supply and perform good drought resilience. Therefore, unfavorable climate conditions may not significantly affect the productivity of these crops. Note that R4 only ranked sixth of eight regions in terms of drought frequency and severity; it exhibited many outliers, possibly caused by large variations in rainfall and air temperature in this region (see Appendix 3). Overall, the three spatial resolutions provided similar drought characteristics information; however, higher resolution datasets exhibited more spatial details in the variation of drought characteristics, demonstrating a higher number of outliers.

Trends of severity and frequency of droughts are presented in Figs. 9 and 10. Spatial patterns of these trends can roughly be characterized as having a north-south contrast, similar to the patterns found in the trends of precipitation and air temperature (Figs. 5 and 6). Both wetting in the northern region and drying in the southern region were found to be most significant based on SPEI. The increasing trend in drought frequency and severity in the southern part is more widespread, with the most significant areas ($p < 0.05$) found in the northern and central part of R8, which might reflect the prevalent decreasing trend of precipitation and the increasing trend of air temperature in the same region.

Table 3

Descriptive statistics of the Mann-Kendall test and Sen's slope for drought frequency in different spatial resolutions (1-, 9-, and 36-km) in eight sub-regions. Significant trends occur when p-value < 0.05.

Spatial Resolution	Description	R1	R2	R3	R4	R5	R6	R7	R8
1-km	n	43,964	43,622	12,071	43,598	36,293	45,503	18,998	31,688
	Sig. Decrease (% of total land)	5.47	27.23	62.80	0.15	–	–	–	–
	Sig. Increase (% of total land)	0.22	–	–	2.51	9.59	2.23	0.01	13.40
	Average Slope (%/year)	-0.28	-0.80	-1.11	0.21	1.14	1.66	1.82	1.42
9-km	n	545	543	150	536	446	565	239	406
	Sig. Decrease (% of total land)	6.06	28.55	66.00	0.19	–	–	–	–
	Sig. Increase (% of total land)	0.37	–	–	2.61	9.19	1.95	0.00	13.55
	Average Slope (%/year)	-0.27	-0.80	-1.12	0.21	1.15	1.69	1.82	1.41
36-km	n	36	33	10	30	29	36	14	23
	Sig. Decrease (% of total land)	5.56	27.27	60.00	–	–	–	–	–
	Sig. Increase (% of total land)	–	–	–	3.33	10.69	5.56	–	17.39
	Average Slope (%/year)	-0.24	-0.78	-1.05	0.00	1.01	1.91	1.71	1.70

Table 4

Same as [Table 3](#) but for drought severity (absolute value).

Spatial Resolution	Description	R1	R2	R3	R4	R5	R6	R7	R8
1-km	n	43,964	43,622	12,071	43,598	36,293	45,503	18,998	31,688
	Sig. Decrease (% of total land)	5.36	29.46	61.94	0.61	–	–	–	–
	Sig. Increase (% of total land)	0.00	–	–	2.77	9.00	1.40	0.27	16.13
	Average Slope (%/year)	-0.07	-0.15	-0.21	0.06	0.22	0.30	0.35	0.27
9-km	n	545	543	150	536	446	565	239	406
	Sig. Decrease (% of total land)	5.50	29.28	65.33	0.75	–	–	–	–
	Sig. Increase (% of total land)	0.00	–	–	2.99	8.74	1.59	0.84	16.26
	Average Slope (%/year)	-0.07	-0.15	-0.21	0.06	0.23	0.31	0.35	0.27
36-km	n	36	33	10	30	29	36	14	23
	Sig. Decrease (% of total land)	2.78	27.27	60.00	3.33	–	–	–	–
	Sig. Increase (% of total land)	–	–	–	3.33	10.34	2.78	–	21.74
	Average Slope (%/year)	-0.06	-0.15	-0.21	0.03	0.21	0.34	0.30	0.30

[Table 3](#) presents descriptive statistics of significant decreasing (increasing) trends in terms of drought frequency in different spatial resolutions during 1989–2018. The drought frequency exhibited a significant reduction in R3 in 62.8 %, 66.0 %, and 60.0 % of total land, based on 1-, 9-, and 36-km, respectively. On the contrary, significant increasing trends in drought frequency were found in the R5 and R8 regions. According to 1-, 9, and 36-km products, drought frequency significantly increased to 9.59 %, 9.19 %, and 10.69 % of the total land in R5, respectively. These magnitudes for R8 regions were 13.40 %, 13.55 %, and 17.39 % of total land, respectively.

Regarding drought severity (absolute values) during 1989–2018, descriptive statistics of significant decreasing (increasing) trends are given in [Table 4](#). A similar observation in drought severity compared to drought frequency, R3 exhibited the most decreasing trends in drought severity, while R5 and R8 experienced the most increasing trends. The proportion of land in decreasing (increasing) trends in drought severity were largely similar to these figures in drought frequency but averaged a difference of around 2%.

5.4. Comparison between PDA estimated from SPEI and actual agricultural record PDA

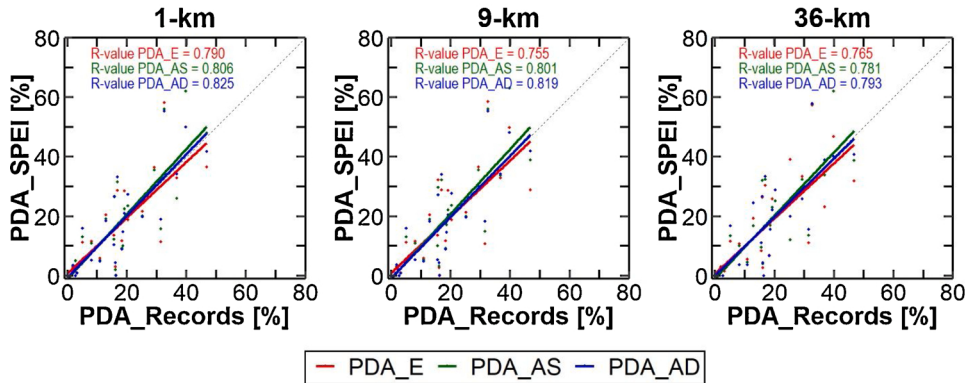
[Fig. 11](#) presents scatterplots between three different PDA estimated from SPEI and that from record data at R4 and R5 regions, during 1989–2014. Overall, the distribution patterns of scattered points of all three different resolution products are similar for both sub-regions. However, the 1-km dataset has a better agreement with the PDAs based on the observed records compared to the coarse-resolution products (9-km and 36-km). The average correlation coefficient (R-value) between the 1-km PDA product and PDA from record data was 0.807. These figures for 9-km and 36-km products were 0.792 and 0.779, respectively.

For each spatial resolution, when we compared PDA estimated from different land cover (PDA-E, PDA-AS, and PDA-AD), there was evidence that the PDA-AD exhibited better agreement with PDA from the data records. First, the slopes from PDA-AD products were closer to the 1:1 line than these slopes from PDA-E and PDA-AS. Second, R-values between PDA-AD and PDA-observation were generally higher than R-values from others.

Overall, a better estimation of percentage drought areas in agricultural lands based on SPEI was found at the higher-resolution dataset and in using dynamic land cover. Note that, using a constant land cover to estimate PDA also provided comparable results with using dynamic land cover.

This validation has a limitation: we only examined PDA_AD in R4 and R5, which had no significant changes in agricultural land over the study period. However, they still provide the first identification of potential usefulness of using dynamic land cover.

(a) R4



(b) R5

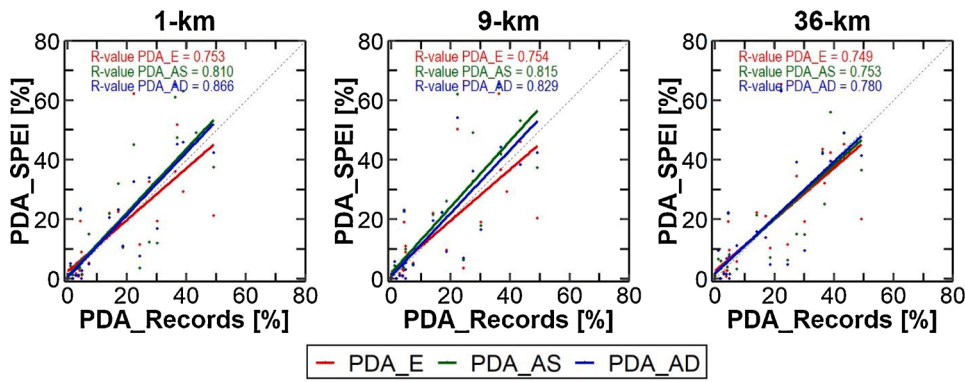


Fig. 11. Comparison of Percentage Drought Area (PDA) estimated from simulated SPEI and observed records in different spatial resolutions (1-, 9-, 36-km) in R4 and R5. The gray dash line denotes a 1-1 line. The bold lines in red, green, and blue are the regression lines between PDA based on SPEI and PDA based on observed records.

5.5. Assessing spatio-temporal dynamics drought from high-resolution data sets

It is important to understand total agricultural land in drought in each month for the past 30 years 1989–2018. In the previous section, 1-km PDA-AD exhibited the best overall among others in terms of estimation of PDA in agricultural land in the R4 and R5 region. Therefore, we used this product to explore the historical agricultural lands in drought conditions over Vietnam during 1989–2018 (Figs. 12 and 13). Generally, droughts in agricultural land throughout sub-regions occurred every 1–2 years, which is in agreement with the conclusions of Hoc (2002). After 2010, the PDA was found less severe in north Vietnam (R1–3), but more severe in south Vietnam (R7–8). During extreme El Niño conditions (1998, 2002, 2005, 2010, and 2014–16), drought nearly occurred in all sub-regions, with PDA up to 100 % in many months. It was also found that extreme drought conditions (high PDA in consecutive months) during El Niño years were more pronounced in sub-regions from R5 toward the south, reflecting the fact that these sub-regions are more sensitive to El Niño conditions. This finding is in agreement with previous studies (Le et al., 2019b). During 1989–2018, agricultural land in Northern Vietnam went through the long-lasting drought in 1989–1991. In R2 and R3 regions, nearly 100 % of agricultural lands were in drought condition during May to December 1989 and May to December 1990. Note that the drought of 1989–1992 may not be directly linked to the El Niño event since the most recent El Niño condition during that time was 1987–1988 and was followed by a La Niña event from 1988–1989. Generally, El Niño conditions cause less rainfall and increased temperatures for Vietnam, while La Niña conditions bring more rainfall. Nguyen and Shaw (2011) also reported droughts in R2, R3 and R5 over the course of 1989–1991.

In Southern Vietnam, during the 30-year study period, the 2014–16 drought caused the worst conditions in agricultural regions in R6, R7, and R8. During summer – autumn – winter period (May–November) of 2014 and 2015, the PDA-AD were estimated at around 80–100 % in R6. This situation is even worse for R7 and R8. Extreme drought conditions (PDA > 80 %) were found in July – August 2013 for these both regions. Agricultural lands in drought conditions were continuously found from May to December (2014); May–December (2015), and January – April (2016). From 1-km PDA-AD, the end of 2014–16 historical drought seems to be at the end of

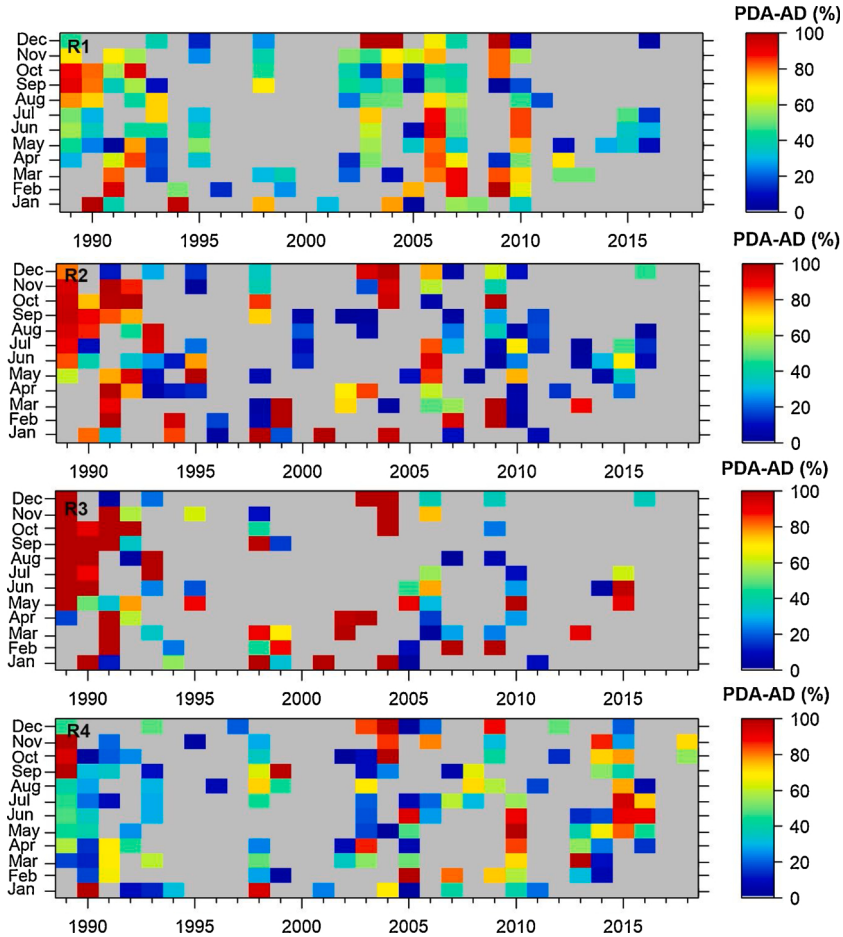


Fig. 12. Percentage drought area for agricultural land using dynamic land cover (PDA-AD) estimated from 1-km spatial resolution in R1, R2, R3, and R4 sub-region based on SPEI during 1989–2018. Gy color denotes no drought condition.

April 2016 (lower PDA observed after that month). This is similar to the actual record as the reports in the losses due to drought for R6 and R8 were also estimated up to April 2016 (Ngo et al., 2020). Up to that month, total land losses due to 2014–16 drought and saline intrusion in R5, R6, and R8 were 242,215 ha paddy rice, 55,651 ha fruit trees, 104,106 ha perennial cash crops, and 4,641 ha aquaculture. More than 400,000 households (equivalent to 1.5 million people) were limited access to drinking water (Ngo et al., 2020).

5.6. Limitations and further studies

Although the MERRA-2 dataset exhibited an overall reasonable relationship with ground observation, it somehow overestimates or underestimates dryness and wetness, as well as often underestimates precipitation and air temperature in Vietnam. Therefore, trend analysis in high error areas should be judged carefully (for example, northern R6 and northern R5). Regarding the validation of PDA from agricultural land, this study could only obtain drought records data in R4 and R5, thus limiting a comprehensive assessment of PDA estimated from SPEI and actual agricultural record PDA for the entire study region.

This study mainly explores drought conditions from a meteorological perspective, which is a combination between precipitation and potential evapotranspiration (i.e. calculated from air temperature). Future study could work on a combination of multi-drought impact factors – actual evapotranspiration, runoff, soil moisture, and soil temperature. For such poorly gauged conditions, land surface models could be a potential approach to obtain these hydrological variables listed above.

In this study, we focused on investigating the applicability of finer resolution disaggregated reanalysis data in drought analysis. It is worth noting that the original spatial resolution of MERRA-2 data is about 50-km, but we intentionally included only 36-km SPEI results in this study because we plan a future comparison of the present research with satellite-based drought indices. Drought indices employing soil moisture data obtained from Soil Moisture Active Passive (SMAP) data will be 36-km because SMAP's original spatial resolution is 36-km (Entekhabi et al., 2010). In the planned future study, the results shown here will be compared with drought indices from satellite-based soil moisture data.

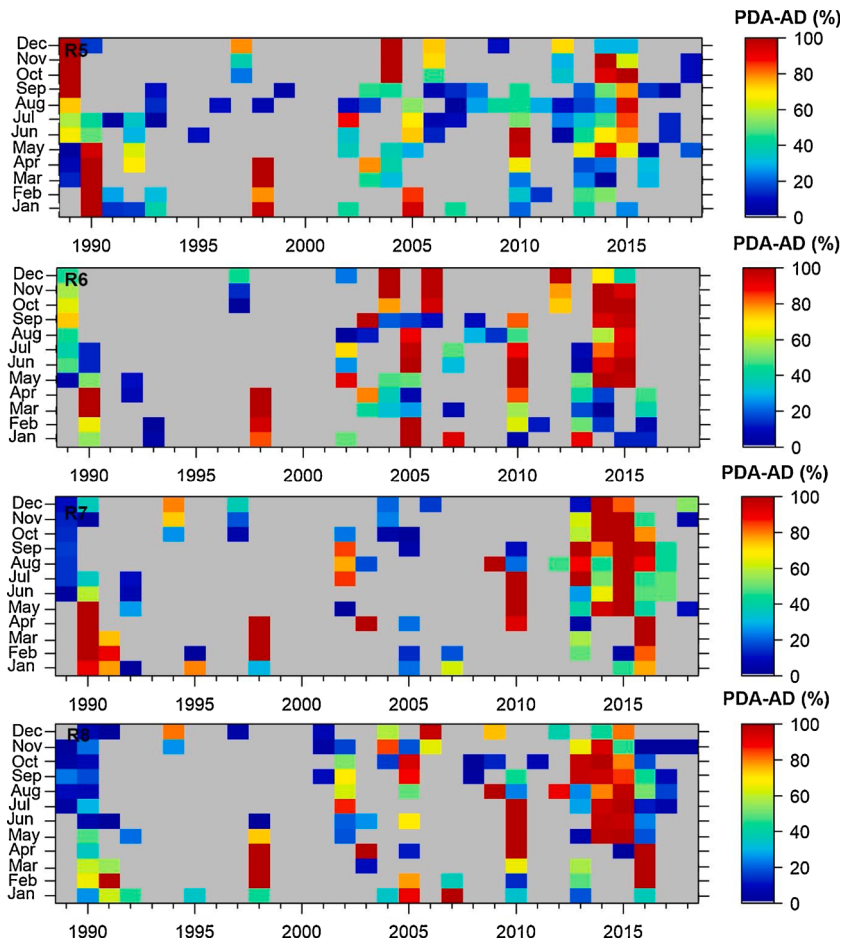


Fig. 13. Percentage drought area for agricultural land using dynamic land cover (PDA-AD) estimated from 1-km spatial resolution in R5, R6, R7, and R8 sub-region based on SPEI during 1989–2018. Gy color denotes no drought condition.

6. Conclusions

In this study, we investigated the ability of a high-resolution re-analysis dataset and dynamic land cover to capture drought conditions over data-sparse areas in Vietnam. The 3-month SPEI was calculated to assess drought trends and its spatio-temporal characteristics using three different spatial resolution datasets from the MERRA-2 datasets on a monthly time scale from 1989 to 2018.

By comparing with in-situ measurements, MERRA-2 exhibited an overall good relationship with these measurements (median R-value and MAE for precipitation: 0.809 and 57.5 mm, respectively; median R-value and MAE for air temperature: 0.977, and 1.14 °C, respectively). It suggests the adequacy of MERRA-2 for studies in Vietnam for drought analysis.

Regarding trend analysis, along with the observed significant trends in precipitation and air temperature, SPEI showed increasing (decreasing) trends in drought severity and frequency in the southern (northern) part of Vietnam. The significant increasing trends of these drought characteristics were found mostly in R5 and R8. The high spatial resolutions of MERRA-2 used in this study allowed us to identify the contrast in drought trends between the northern (wetting/decreasing) and southern (drying/increasing) parts of Vietnam, which are generally shown in coarser climate model simulations.

We designed an experiment which compared the percentage drought area (PDA) estimated based on different land use data sets with PDA from observed records. Overall, the results support the hypothesis that (1) Higher spatial resolution of drought indices, help to accurately characterize and monitor drought events, and (2) PDA using dynamic land cover scenarios results in better agreement with the observed records.

Over the 30-year study period, southern Vietnam underwent unfavorable climate conditions, exhibiting a reduction in rainfall and an increase in temperature which consequently increased the risk of drought frequency and severity. In this region of Vietnam, the 2014–16 drought seems to have produced the worst conditions in terms of temporal duration and spatial extent.

With the advent of higher spatial resolution data sets, specifically for soil moisture (Fang et al., 2018; Kim and Lakshmi, 2018; Narayan and Lakshmi, 2008) add information to ecohydrology (Billah et al., 2015; Hong et al., 2007; Lakshmi et al., 2011) and help to understand the connectivity between hydrology, meteorology and ecology.

In conclusion, this study emphasizes the feasibility of drought analysis using re-analysis datasets in areas where observations are scarce. As we currently have a wide range of re-analysis datasets produced by different institutions, we expect more accurate global-scale drought monitoring with high-resolution model datasets to become possible in future studies.

CRediT authorship contribution statement

Manh-Hung Le: Conceptualization, Methodology, Software, Validation, Formal analysis, Investigation, Resources, Data curation, Writing - original draft, Writing - review & editing, Visualization. **Hyunglok Kim:** Conceptualization, Methodology, Software, Formal analysis, Investigation, Resources, Data curation, Writing - original draft, Writing - review & editing, Supervision, Funding acquisition. **Heewon Moon:** Conceptualization, Methodology, Formal analysis, Investigation, Writing - original draft, Writing - review & editing. **Runze Zhang:** Formal analysis, Investigation, Writing - original draft, Writing - review & editing. **Venkataraman Lakshmi:** Conceptualization, Formal analysis, Investigation, Supervision, Project administration, Funding acquisition. **Luong-Bang Nguyen:** Methodology, Investigation, Resources, Data curation.

Declaration of Competing Interest

The authors report no declarations of interest.

Acknowledgment

We acknowledge funding from the NASA Terrestrial Hydrology Program (Program Manager Jared Entin, grant NNX12AP75G). Acknowledgment funding is also given for Thuyloi University for providing ground observation datasets. The authors thank the teams from NASA, SERVIR-Mekong, for making their datasets accessibly. Special thanks are also given to VMHA, MRC, JICA, and MARD for their ground observation data.

Appendix A. Supplementary data

Supplementary material related to this article can be found, in the online version, at doi:<https://doi.org/10.1016/j.ejrh.2020.100767>.

References

- Arsenault, K.R., et al., 2018. The Land surface Data Toolkit (LDT v7. 2)-a data fusion environment for land data assimilation systems. *Geosci. Model. Dev.* 11 (9), 3605–3621.
- Billah, M.M., et al., 2015. A methodology for evaluating evapotranspiration estimates at the watershed-scale using GRACE. *J. Hydrol.* 523, 574–586.
- Chen, H., Sun, J., 2015. Changes in drought characteristics over China using the standardized precipitation evapotranspiration index. *J. Clim.* 28 (13), 5430–5447. <https://doi.org/10.1175/jcli-d-14-00707.1>.
- Dai, A., 2011. Drought under global warming: a review. *Wiley Interdiscip. Rev. Clim. Change* 2 (1), 45–65.
- Diem, J.E., Ryan, S.J., Hartert, J., Palace, M.W., 2014. Satellite-based rainfall data reveal a recent drying trend in central equatorial Africa. *Clim. Change* 126 (1–2), 263–272.
- Entekhabi, D., et al., 2010. The soil moisture active passive (SMAP) mission. *Proc. IEEE* 98 (5), 704–716.
- Fang, B., Lakshmi, V., Bindlish, R., Jackson, T.J., 2018. Downscaling of SMAP soil moisture using land surface temperature and vegetation data. *Vadose Zone J.* 17 (1), 1–15.
- Ganguli, P., Ganguly, A.R., 2016. Space-time trends in US meteorological droughts. *J. Hydrol. Reg. Stud.* 8, 235–259.
- Gelaro, R., et al., 2017. The modern-era retrospective analysis for research and applications, version 2 (MERRA-2). *J. Clim.* 30 (14), 5419–5454.
- Gocic, M., Trajkovic, S., 2014. Analysis of trends in reference evapotranspiration data in a humid climate. *Hydrol. Sci. J. Des Sci. Hydrol.* 59 (1), 165–180.
- Golian, S., Javadian, M., Behrangi, A., 2019. On the use of satellite, gauge, and reanalysis precipitation products for drought studies. *Environ. Res. Lett.* 14 (7), 075005.
- Greve, P., et al., 2014. Global assessment of trends in wetting and drying over land. *Nat. Geosci.* 7 (10), 716–721.
- Herold, N., Kala, J., Alexander, L., 2016. The influence of soil moisture deficits on Australian heatwaves. *Environ. Res. Lett.* 11 (6), 064003.
- Hirsch, R.M., Slack, J.R., 1984. A nonparametric trend test for seasonal data with serial dependence. *Water Resour. Res.* 20 (6), 727–732.
- Hoc, D., 2002. Drought and Its Mitigation Measures. Agricultural Publishing House, Hanoi, Vietnam.
- Hoerling, M., et al., 2012. On the increased frequency of Mediterranean drought. *J. Clim.* 25 (6), 2146–2161.
- Hong, S., Lakshmi, V., Small, E.E., 2007. Relationship between vegetation biophysical properties and surface temperature using multisensor satellite data. *J. Clim.* 20 (22), 5593–5606.
- Joshi, S., Garbrecht, J., Brown, D., 2019. Observed spatiotemporal trends in intense precipitation events across United States: applications for stochastic weather generation. *Climate* 7 (3), 36.
- Kawase, H., et al., 2010. Physical mechanism of long-term drying trend over tropical North Africa. *Geophys. Res. Lett.* 37 (9).
- Kendall, M.G., 1938. A new measure of rank correlation. *Biometrika* 30 (1/2), 81–93.
- Kim, H., Lakshmi, V., 2018. Use of Cyclone Global Navigation Satellite System (CYGNSS) observations for estimation of soil moisture. *Geophys. Res. Lett.* 45 (16), 8272–8282.
- Krishnan, R., et al., 2016. Deciphering the desiccation trend of the South Asian monsoon hydroclimate in a warming world. *Clim. Dyn.* 47 (3–4), 1007–1027.
- Kumar, S.V., et al., 2006. Land information system: an interoperable framework for high resolution land surface modeling. *Environ. Model. Softw.* 21 (10), 1402–1415.
- Lakshmi, V., Hong, S., Small, E.E., Chen, F., 2011. The influence of the land surface on hydrometeorology and ecology: new advances from modeling and satellite remote sensing. *Nord. Hydrol.* 42 (2–3), 95–112.

- Le, H.M., et al., 2019a. A Comparison of Spatial–Temporal Scale Between Multiscalar Drought Indices in the South Central Region of Vietnam, Spatiotemporal Analysis of Extreme Hydrological Events. Elsevier, pp. 143–169.
- Le, P.V., Phan-Van, T., Mai, K.V., Tran, D.Q., 2019b. Space-time variability of drought over Vietnam. *Int. J. Climatol.* 39 (14), 5437–5451.
- Le, M.-H., Lakshmi, V., Bolten, J., Du Bui, D., 2020. Adequacy of satellite-derived precipitation estimate for hydrological modeling in Vietnam Basins. *J. Hydrol.* 124820.
- López-Moreno, J.I., et al., 2013. Hydrological response to climate variability at different time scales: a study in the Ebro basin. *J. Hydrol.* 477, 175–188. <https://doi.org/10.1016/j.jhydrol.2012.11.028>.
- Mann, H.B., 1945. Nonparametric tests against trend. *Econometrica: Journal of the Econometric Society* 245–259.
- Mazdiyasi, O., AghaKouchak, A., 2015. Substantial increase in concurrent droughts and heatwaves in the United States. *Proc. Natl. Acad. Sci.* 112 (37), 11484–11489.
- McCarty, W., et al., 2016. MERRA-2 Input Observations: Summary and Assessment. NASA Tech. Rep. Series on Global Modeling and Data Assimilation, NASA/TM-2016-104606, p. 64, 46.
- Miralles, D.G., Gentine, P., Seneviratne, S.I., Teuling, A.J., 2019. Land-atmospheric feedbacks during droughts and heatwaves: state of the science and current challenges. *Ann. N. Y. Acad. Sci.* 1436 (1), 19.
- Mondal, A., Khare, D., Kundu, S., 2015. Spatial and temporal analysis of rainfall and temperature trend of India. *Theor. Appl. Climatol.* 122 (1–2), 143–158.
- Narayan, U., Lakshmi, V., 2008. Characterizing subpixel variability of low resolution radiometer derived soil moisture using high resolution radar data. *Water Resour. Res.* 44 (6).
- Ngo, V.Q., et al., 2020. Water Resources Engineering (in Vietnamese). Bach Khoa Publishing House - Hanoi, Hanoi.
- Nguyen, D.N., Nguyen, T.H., 2004. Climate and Climate Resources in Vietnam (in Vietnamese). Agricultural Publishing House, Hanoi, Vietnam.
- Nguyen, H., Shaw, R., 2011. Drought risk management in Vietnam. Chapter 8 Droughts in Asian Monsoon Region. Emerald Group Publishing Limited, Bingley, UK, pp. 141–161.
- Nguyen, D.Q., Renwick, J., McGregor, J., 2014. Variations of surface temperature and rainfall in Vietnam from 1971 to 2010. *Int. J. Climatol.* 34 (1), 249–264.
- Orlowsky, B., Seneviratne, S.I., 2013. Elusive drought: uncertainty in observed trends and short-andlong-term CMIP5 projections. *Hydrol. Earth Syst. Sci.* 17 (5), 1765–1781.
- Phan, V.-T., Ngo-Duc, T., 2009. Seasonal and interannual variations of surface climate elements over Vietnam. *Clim. Res.* 40 (1), 49–60.
- Raziei, T., Bordi, I., Pereira, L.S., 2013. Regional drought modes in Iran using the SPI: the effect of time scale and spatial resolution. *Water Resour. Manag.* 27 (6), 1661–1674.
- Rojas, O., Vrielink, A., Rembold, F., 2011. Assessing drought probability for agricultural areas in Africa with coarse resolution remote sensing imagery. *Remote Sens. Environ.* 115 (2), 343–352.
- Rutten, M., Van Dijk, M., Van Rooij, W., Hilderink, H., 2014. Land use dynamics, climate change, and food security in Vietnam: a global-to-local modeling approach. *World Dev.* 59, 29–46.
- Sen, P.K., 1968. Estimates of the regression coefficient based on Kendall's tau. *J. Am. Stat. Assoc.* 63 (324), 1379–1389.
- Sharma, S., Mujumdar, P., 2017. Increasing frequency and spatial extent of concurrent meteorological droughts and heatwaves in India. *Sci. Rep.* 7 (1), 1–9.
- Sheffield, J., Wood, E.F., 2008. Global trends and variability in soil moisture and drought characteristics, 1950–2000, from observation-driven simulations of the terrestrial hydrologic cycle. *J. Clim.* 21 (3), 432–458.
- Sheffield, J., Wood, E.F., Roderick, M.L., 2012. Little change in global drought over the past 60 years. *Nature* 491 (7424), 435–438.
- Simpson, E.H., 1949. Measurement of diversity. *Nature* 163 (4148), 688–688.
- Svoboda, M., Hayes, M., Wood, D., 2012. Standardized Precipitation Index User Guide. World Meteorological Organization Geneva, Switzerland.
- Thornthwaite, C.W., 1948. An approach toward a rational classification of climate. *Geogr. Rev.* 38 (1), 55–94.
- Tuan, B.M., 2019. Extratropical forcing of submonthly variations of rainfall in Vietnam. *J. Clim.* 32 (8), 2329–2348.
- Valdes-Abellan, J., Pardo, M., Tenza-Abril, A.J., 2017. Observed precipitation trend changes in the western Mediterranean region. *Int. J. Climatol.* 37, 1285–1296.
- Van Der Linden, R., Fink, A.H., Phan-Van, T., Trinh-Tuan, L., 2016. Synoptic-dynamic analysis of early dry-season rainfall events in the Vietnamese central highlands. *Mon. Weather. Rev.* 144 (4), 1509–1527.
- Van Loon, A.F., et al., 2016. Drought in a Human-modified World: Reframing Drought Definitions, Understanding, and Analysis Approaches.
- Velpuri, N., Senay, G., 2013. Analysis of long-term trends (1950–2009) in precipitation, runoff and runoff coefficient in major urban watersheds in the United States. *Environ. Res. Lett.* 8 (2), 024020.
- Vicente-Serrano, S.M., Beguería, S., López-Moreno, J.I., 2010. A multiscalar drought index sensitive to global warming: the standardized precipitation evapotranspiration index. *J. Clim.* 23 (7), 1696–1718.
- Vu, T., Mishra, A., 2016. Spatial and temporal variability of standardized precipitation index over Indochina peninsula. *Cuadernos de Investigación Geográfica* 42 (1), 221–232.
- Vu, T.M., Raghavan, S.V., Lioung, S.Y., Mishra, A.K., 2018. Uncertainties of gridded precipitation observations in characterizing spatio-temporal drought and wetness over Vietnam. *Int. J. Climatol.* 38 (4), 2067–2081.
- Vu-Thanh, H., Ngo-Duc, T., Phan-Van, T., 2014. Evolution of meteorological drought characteristics in Vietnam during the 1961–2007 period. *Theor. Appl. Climatol.* 118 (3), 367–375.
- Wang, F., Wang, Z., Yang, H., Zhao, Y., 2018. Study of the temporal and spatial patterns of drought in the Yellow River basin based on SPEI. *Sci. China Earth Sci.* 61 (8), 1098–1111. <https://doi.org/10.1007/s11430-017-9198-2>.
- Winkler, K., Gessner, U., Hochschild, V., 2017. Identifying droughts affecting agriculture in Africa based on remote sensing time series between 2000–2016: rainfall anomalies and vegetation condition in the context of ENSO. *Remote Sens. (Basel)* 9 (8), 831.
- Yuan, X., et al., 2019. Anthropogenic shift towards higher risk of flash drought over China. *Nat. Commun.* 10 (1), 1–8.
- Yue, S., Pilon, P., Phinney, B., Cavadias, G., 2002. The influence of autocorrelation on the ability to detect trend in hydrological series. *Hydrol. Process.* 16 (9), 1807–1829.
- Zhang, X., et al., 2013. Enhanced poleward moisture transport and amplified northern high-latitude wetting trend. *Nat. Clim. Chang.* 3 (1), 47–51.
- Zhu, Y., Wang, W., Singh, V.P., Liu, Y., 2016. Combined use of meteorological drought indices at multi-time scales for improving hydrological drought detection. *Sci. Total Environ.* 571, 1058–1068.
- Zuo, D., et al., 2018. Spatiotemporal patterns of drought at various time scales in Shandong Province of Eastern China. *Theor. Appl. Climatol.* 131 (1–2), 271–284.